Journal of Renewable Materials

Tech Science Press

DOI: 10.32604/jrm.2022.023621

ARTICLE

Preparation and Properties of Chinese Lacquer Modified by Methylolureas

Qiang Xiao[1,2], Yanjun Cao[1,2], Hailu Tan[1,2], Qiaoling Feng[1,2], Xinyue Gu[1,2], Jianhua Lyu[1,2], Hui Xiao[1,2], Ming Chen[1,2,*] and Yuzhu Chen[1,2,*]

[1]College of Forestry, Sichuan Agricultural University, Chengdu, 611130, China

[2]Wood Industry and Furniture Engineering Key Laboratory of Sichuan Provinvial Department of Education, Sichuan Agricultural University, Chengdu, 611130, China

[*]Corresponding Authors: Ming Chen. Email: chenming@sicau.edu.cn; Yuzhu Chen. Email: populus_zhu@163.com

Received: 06 May 2022 Accepted: 18 July 2022

ABSTRACT

In this study, different molar of methylolureas (MMU) were used to improve the properties and drying speed of the raw lacquer (RL). The drying time, gloss, pencil hardness and impact resistance of the lacquer film were tested. The thermal behaviors and chemical structures of the lacquer membrane were also discussed by thermal gravimetric analysis (TGA), fourier infrared spectrometer (FT-IR) and nuclear magnetic resonance (NMR) analysis, respectively. The results demonstrated that lower molar ratio MMU can significantly improve the properties of lacquer. The TGA analysis showed that the modified lacquer had high thermal stability than that of the control. The FT-IR and 13C NMR analysis revealed that the structures of the modified lacquer were significantly improved by cross-linking with the hydroxymethyl groups and methylene methyl ethers of MMU. In addition, through scanning electron microscopy (SEM) characterization, it was found that the introduction of MMU can effectively improve the surface smoothness of the lacquer film.

KEYWORDS

Raw lacquer; methylolureas; properties; thermal behavior; chemical structure

1 Introduction

Raw lacquer (RL) is a natural environmentally friendly coating derived from lacquer tree with a long history of use [1,2]. RL is a water in oil emulsion, whose component including urushiol (60%~80%), water (20%~30%), plant gummy substance (5%~7%), glycoproteins (~2%) and laccase (<1%) [2,3]. The main film-forming substance of RL is urushiol, which can be divided into three main kinds of catechol derivatives depend on the different side chain structure on catechol ring. The first and second side chain structures have a chain of 15 and 17 carbons at the no. 3 position of catechol ring, respectively, while the third side chain structure has a chain of 17 carbons at the no. 4 position of catechol ring [1,4].

According to reports, during the polymerization process of lacquer sap, the quinone free radicals are produced from the lipid components (mainly urushiol) by the catalyzed effect of laccase, which then undergo radical transfer and coupling reactions [1,3,5,6]. When the monomer concentration is below 30%, the unsaturated side chain autooxidation reaction occurs, promoting urushiol curing [1,3].

RL is widely used in many fields because of its water impermeability, high heat resistance, excellent gloss, environmental friendliness, chemical resistance, strong durability, and corrosion resistance [2,7,8]. However, the widespread application of RL is restricted by the following three disadvantages. (i) The first one is the slow drying speed. The curing process of urushiol involves laccase catalyzed and aerobic oxidation polymerization, and both of which require a long drying time and special drying conditions (relative humidity of 80%–90% and temperature of 20°C–30°C). As a polymerization accelerator of urushiol, laccase plays a crucial role in this process and restricts the applications and development of lacquer. What's more, laccase will lose its activity during a long period of storage, resulting in the inactivation of RL [4,8,9]. (ii) Hard coating. The lacquer solutions are water-oil emulsion which makes it difficult to apply to the objects [10,11]. (iii) Hypersensitivity. Due to the existence of phenol hydroxyl group in urushiol, people can easily cause allergies by touching or smelling RL [12].

The process of lacquer film formation is the polymerization of urushiol monomers to form polymers. There are many substances that can increase its network structure, such as GO, MWCNTs, nano-silica, nano-titania, etc. [13–15]. These nanomaterials can promote the formation of network structure of urushiol. However, few inorganic substances can promote the network structure of urushiol, inspired by urushiol-formaldehyde polymer (UFP), methylol urea (MMU) rich in hydrophilic amino groups and methylol groups can promote urushiol formation of the network structure. In this paper, methylol urea (MMU) was synthesized with different molar ratios (F/U) of formaldehyde and urea, and the molar ratio and addition amount of MMU were optimized by combining the comprehensive properties and chemical structure of the modified RL. The RL before and after modification were analyzed by FT-IR and NMR.

2 Experimental

2.1 Materials

Formaldehyde aqueous solution (37% concentration), urea (99%) and NaOH were purchased from Chengdu Kelong Chemicals Co., Ltd. (China). RL was purchased from Chengdu Lacquer Craft Factory Co., Ltd. (China). Its main structure was shown in Scheme 2. All chemicals were analytical reagent grade.

2.2 Methods

2.2.1 Synthesis of MMU

MMU was produced by formaldehyde and urea with molar ratio of 0.30, 0.50, 0.70, and 1.00, respectively. Formaldehyde and urea were placed in a tri-neck flask equipped with agitator, thermometer, and reflux condenser. Subsequently, the pH value was adjusted to 8.0–9.0 with NaOH (50% aqueous solutions). Then the mixture was heated to 90°C within 40 min and maintain it for 30 min, and then cooled to room temperature.

2.2.2 Preparation of MMU Modified RL

Different molar ratios of MMU were added to RL at 40°C and stirred for 3 h [16–18]. RL modified by MMU with mole ratios of 0.30, 0.50, 0.70 and 1.00 were named LMU1, LMU2, LMU3, and LMU4, respectively.

2.2.3 Determination of Drying Time

The drying time were tested according to the Chinese national standard GB/T 1727-1992. The lacquers were dried under the conditions of 30°C and 80% relative humidity, and of the lacquer film was tested every five minutes half an hour later. The filter paper was putted on the tinplate with lacquer film, the filter paper didn't flop when the tinplate flipped 180° after 30 s, then this time was HD [19]. The process was shown in Fig. 1.

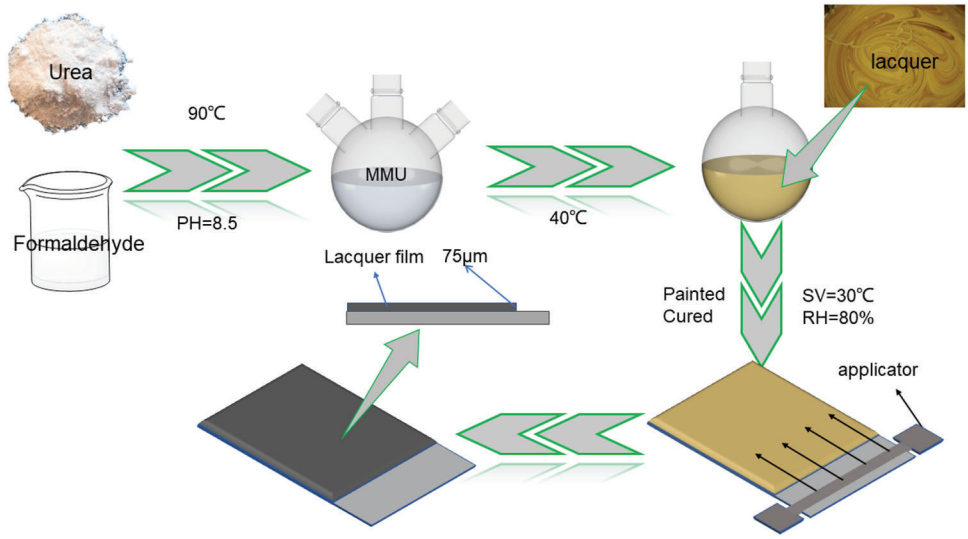

Figure 1: The preparation process of LMU

2.2.4 Performance Test

The completely dried lacquer film was placed at room temperature for seven days before performance test. Hardness, impact resistance and glossiness of lacquer film were tested by pencil hardness tester (QHQ-A), lacquer film impactor (CQJ-II) and glossmeter (WGG60-Y4), according to the Chinese national standard GB/T 6739-2006, GB/T 1732-2020 and GB/T 9754-2007, respectively.

2.2.5 Thermal Gravimetric Analysis

LMU1 with addition amount of 1 wt%, 3 wt%, 5 wt% and 7 wt% were used to thermogravimetric analysis. All samples were stirred at 40°C for 3 h before testing. Non-isothermal measurements were performed with thermogravimetric (TG) instrument (TG 209F3, Netzsch) at heating rates of 10 °C/min from 30°C to 800°C under nitrogen environment.

2.2.6 FT-IR Spectra and Nuclear Magnetic Resonance Spectrum Analysis

The optimized LMU1-3%, RL and MMU were subjected to infrared measurement and nuclear magnetic measurement. All samples were stirred at 40°C for 3 h before testing. The infrared spectrum (IR) were tested by a spectrometer (Thermo Scientific Nicolet is5, Thermo Fisher) and tested in a dry environment at room temperature. The wavenumber range is from 400 cm^{-1} to 4000 cm^{-1}.

^{13}C NMR spectra were recorded by Bruker 600 M. The spectrum of the samples runs a scanning frequency of 600 M Hz. Tetramethylsilane was used as the internal standard. The sap of RL and LMU were extracted with tetrahydrofuran and first then removed the tetrahydrofuran below 40°C, and then dissolved the sample by $CDCl_3$.

2.2.7 SEM

The scanning electron microscope test of LMU1 series lacquer films was carried out by scanning electron microscope (SEM) (Zeiss Sigma 300, Germany) and the surface morphologies of lacquer films and mixed paint films were characterized.

2.2.8 Chemical Resistance Test

The RL and LMU1 were placed in 10% H_2SO_4, 10% NaOH, 10% NaCl and 95% C_2H_5OH. After 7 days, the lacquer film was observed for wrinkling and peeling.

3 Results and Discussion

3.1 Effect of MMU Molar Ratio on the Performance RL

Effect of MMU molar ratio on the properties of RL were shown in Table 1. It can be observed that with the MMU molar ratio increasing, the gloss and pencil hardness decrease. The comprehensive performance of LMU increase with decrease of molar ratio of MMU.

Table 1: The properties of RL modified by different molar ratio of MMU with 3 wt% loading level

Loading level	Sample	Molar ratio (F and U)	HD (minute)	Gloss (GU)	Hardness	Impact resistance (cm)
3.0 wt%	RL	–	190	110.3	3H	15
	LMU1	0.30	165	147.3	5H	40
	LMU2	0.50	200	112.2	3H	40
	LMU3	0.70	200	108.2	4B	50
	LMU4	1.00	185	84.3	2B	50

Due to the moisture shows a vital role during the curing process of the lacquer membrane, the higher humidity environment was beneficial to active the laccase which was indispensable to promote the oxidation of the urushiol under its catalyzed effect [10]. First of all, the PH value of MMU was alkaline, which reduced the concentration of hydrogen ion in the lacquer solution and promoted the function of laccase to accelerate the drying of film [7,20]. MMU is rich in hydrophilic amino and hydroxymethyl groups. On one side, amino groups are very hydrophilic, which can make the urushiol molecules disperse evenly and cross-link rapidly, and effectively speed up the drying time and improve impact resistance. On the other side, the auto-condensation among the hydroxymethyls would produce more ether linkages, whose dendritic structure or cross-linkage structure would restrict the movement or evaporation of the free water leading to more water remained in the system and prolonged the drying time [21]. The groups of amino and hydroxymethyls showed constraint effect on drying time with each other in the LMU system. The lower the molar ratio of MMU, the higher the ratio of amino groups. When the molar ratio of MMU is 0.30, the HD of LUM1 is shorter than that of RL. However, with the increase of MMU molar ratio, the increase of water in the system leads to the decrease of gloss and hardness of the film.

3.2 Effect of MMU Loading Level on the Performance of RL

Comprehensive performance of LMU1 with different loading level were shown in Table 2. It could be seen that the optimal addition amount of MMU was 3.0%, and the HD, gloss, pencil hardness and impact resistance of which were significantly better than those of RL. This was due to the combined effect of hydrogen ion concentration, hydroxymethyl and amino groups. When the loading level of MMU is less than 3.0%, the amino groups and the value of PH play a major role in the performance of the RL film. However, because the self-oxidation of urushiol is restricted by hydroxylmethyl, the content of hydroxylmethyl plays a dominant role in affecting the performance of the RL film with the increase of the MMU addition amount.

The chemical medium resistance of LMU1 with different ratio were shown in Table 3. The permittivity conditions were summarized in Table 3. The lacquer film without wrinkling and peeling was indicated by "+", the lacquer film with wrinkling and peeling was indicated by "-", and the lacquer film with slight wrinkling and peeling was indicated by "±". The results showed that both RL and LMU1 had strong corrosion resistance in 10% H_2SO_4 and 10% NaCl. In terms of alkali resistance, after adding MMU, the alkali resistance of RL was significantly improved. The RL showed obvious peeling and wrinkling after

soaking in alkaline solution. When the loading level of MMU is 3.0%, the wrinkling and peeling phenomena disappeared completely. This was due to the dendritic structure of the MMU molecules providing many polyions, thereby improving the alkali resistance of the film. However, when the amount of MMU was 7.0%, the modified lacquer was wrinkled and peeled. This was due to the excessive addition of MMU, resulting in a certain amount of methylol not participating in the reaction, and the increase in hydroxyl content, reducing the alkali resistance of the lacquer film. In terms of resistance to ethanol solutions, the load-bearing capacity of the lacquer film was obviously improved after adding MMU. Although the lacquer film had cured, there were still small molecules such as urushiol dimer. This small molecule was easily soluble in ethanol, so it will wrinkle and peel, but the ether bond in MMU made urushiol form a tight network structure, reducing the content of urushiol dimer, making the modified lacquer film had a certain resistance ethanol solution property.

Table 2: The properties of LMU1 with different ratio

Sample name	Molar ratio (F and U)	Loading level	HD (minute)	Gloss (GU)	Hardness	Impact resistance (cm)
RL		–	190	110.3	3H	15
LMU1	0.30	1.0%	180	137.6	4H	50
		3.0%	165	147.3	5H	40
		5.0%	195	146.6	3H	50
		7.0%	340	136.5	B	50

Table 3: The chemical medium resistance of LMU1 with different ratio

Contents (%)	0	1	3	5	7
10% H_2SO_4	+	+	+	±	–
10% NaOH	–	±	+	±	–
95% C_2H_5OH	–	–	+	+	+
10% NaCl	+	+	+	+	+

3.3 Thermogravimetric Analysis

The TG-DTG curves of LMU1 with different loading level were exhibited in Fig. 2. The peak temperature, the relative mass loss rate during the different temperatures ranges, and char residuals at 800°C were shown in Table 4.

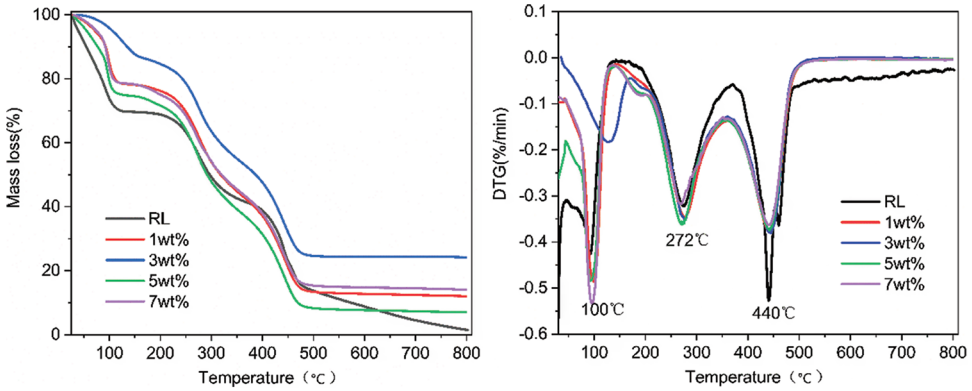

Figure 2: The TG-DTG curves of LMU1 with different loading level

Table 4: The relationship analysis between temperature and mass loss from TG-DTA curves of RL, LMU1

Sample	Loading level	Peak temperature °C			Corresponding mass loss %				Char residual at 800°C
		I	II	III	Temperature °C				
					RT-200	200–370	370–500	500–800	
RL	–	93	274	440	31.188	27.489	27.589	11.975	1.759
LMU1	1	96	274	442	23.785	34.111	28.715	1.351	12.074
	3	126	274	440	15.382	32.182	27.788	0.413	24.230
	5	95	270	442	28.383	35.076	28.198	1.259	7.016
	7	95	270	440	24.912	32.213	27.452	1.230	14.119

The mass loss trend of all samples is basically the same, the biggest difference is that RL has a significant mass loss when the temperature is higher than 500°C, while the modified RL basically has no mass loss. From the TG and DTG curves, the pyrolysis process of RL and LMU can be divided into four stages. The first stage temperature was between room temperature and 200°C. In this stage, the mass loss is mainly due to evaporation of water. The highest degradation rate was at 100°C. The second stage temperature was between 200°C and 370°C, the peak degradation occurs at 272°C, which mainly due to the linkages of the polysaccharides and glycoproteins were broken down at this stage [2]. The temperature of the third stage was 370°C to 500°C. The degradation of the oligomer and polymer in urushiol was the main reaction in this stage. The peak temperature of degradation was about 440°C. The last stage was 500°C to 800°C. the modified RL basically has no mass loss while RL has a significant mass loss in this stage [17].

In the first stage, the mass loss of the RL was 30% due to the evaporation of water. The mass loss of the LMU were lower than that of the control. In addition, the complex polycondensation would happen in this stage. One kind was the self-condensation reaction among the methylolureas or between the methylolureas and aminos would happen between 80°C and 100°C, leading to the production of the ether bond. And the other kind was the addition reaction between hydroxymethyls and benzene ring of the urushiol, and the co-condensation between the hydroxymethyphenols and the methylolureas at 170°C~176°C, self-condensation of hydroxymethyphenols at 140°C~145°C. The ether groups would break down into the di-methylene bonds and free formaldehyde with the increased temperature [22].

At second stage, the mass loss of the RL was about 27%. However, the ingredient of plant gummy substance and glycoproteins in lacquer was about 10% [2,3]. In Table 4, it can be indicated that the corresponding mass loss of LMU between 200°C to 370°C was about 30%–35%. Therefore, apart from the polysaccharides and glycoproteins, the monomer and oligomer of lacquer were also degraded in this stage. In addition, the mass loss of the LMU was higher than that of the control, the reason for this variation was that the branching structure of the MMU may react with many long aliphatic isomers or other minor phenolic liquids in the urushiol, such as 3-substitued catechols with n = 15 carbon chains and conjugated triene, resulting in the higher branching degree of the LMU, the higher sensitivity to temperature and the higher thermal stability of the film [10]. When the length of alkyl chain was longer, or the content of alkyl substituted phenol contained was higher in polymer, the significant sharp decline in weight would be easier happen.

In the third stage, there is no obvious difference between the mass loss of modified RL and unmodified RL. In the last stage, the mass loss of RL is close to 12%, while the mass loss of modified raw lacquer is less than 3.3%. However, when the MMU added into the RL, the loss rate of urushiol was obviously reduced [23,24]. When the temperature reached 800°C, the char residual rate of modified raw lacquer was much

higher than that of RL, the char residual of RL and LMU1-3% were 2% and 24%, respectively. These results were identical with the analysis of comprehensive performance.

The TG-DTG curves of lacquer film of RL and LMU1-3% were shown in Fig. 3. The peak degradation rate of LUM1 was lower than that of RL indicating that LUM had better thermal stability than RL, which might be due to the addition of MMU promoting the cross-linking reaction of RL.

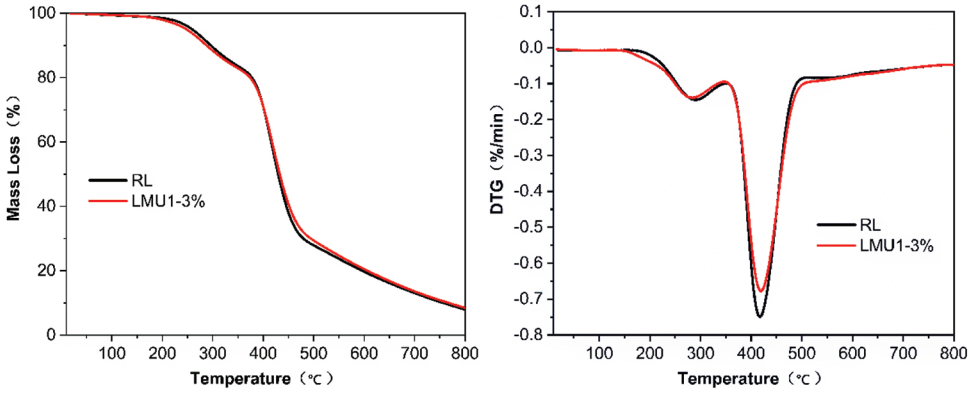

Figure 3: The TG-DTG curves of lacquer film of RL and LMU1-3%

3.4 FT-IR Spectra Analysis

The FT-IR spectra of RL, LMU1-3% were shown in Fig. 4. Based on these absorption peaks, there were mainly five functional groups. They were O-H, C-H on side chain, C=O, aromatic hydrocarbon and conjugated triplex respectively. In Fig. 3, the absorption peaks at 3300–3400, 1360, 1281, 1195 and 734 cm^{-1} come from the α-oxyhydrogen tensile vibration, β-oxyhydrogen vibration, aromatic amines, carbon oxygen Tensile vibration and hydrogen oxygen out of plane deformation vibration of urushiol, respectively [3,25]. The next absorption peaks at 3021, 2800–2975, 1475 and 1070–1110 cm^{-1} were caused by the stretching motion of C-H, which were respectively derived from the stretching vibration of C-H on urushiol, the stretching vibration of C-H on branched chain, the shear deformation vibration of CH_2 and the in-plane deformation vibration of monosubstituted C-H. The absorption peak at 1621 cm^{-1} and 1500–1600 cm^{-1} were mainly from the stretching motion of C=O and stretching vibration of benzene ring. The absorption peak at 988 cm^{-1} was derived from conjugated triplex [26,27]. In Fig. 4B, there were mainly three function structures. The absorption peaks at 3200–3500, 1650 and 1000–1200 cm^{-1} were from O-H and N-H stretching vibrations, carbonyl stretching and hydroxymethyl vibrations and alcohol stretching vibrations, respectively.

In Fig. 4A, the absorption peaks at 3400, 2975 and 734 cm^{-1} of LMU1-3% were significantly enhanced, it seemed that the enzymatic polymerization had occurred, and the oligomers were formed. The side chains in urushiol and phenolic hydroxyl had converged to be oligomer [28]. And then, the absorption peaks at 1070–1110 cm^{-1} and 988 cm^{-1} of LMU1-3% were slightly reduced, which illustrated the structure of the conjugated alkatriene was decreased. This phenomenon further illustrated that the opening of the carbon-carbon double bond and the hydroxyl group on urushiol had combined. In addition, the intensity of the absorption peak at 1281 cm^{-1} increases, indicating that the amino group reacted with the phenol ring of urushiol [29]. It also can be seen that the O-H and C=O absorption areas of LMU1 were slightly larger than that of RL, which mainly due to the hydroxyl group in MMU and urushiol was oxidized to urushiol quinone, respectively [30]. Another possible reason was the combine of the hydroxyl groups on the phenyl ring and the C=C bonds in side chain [31].

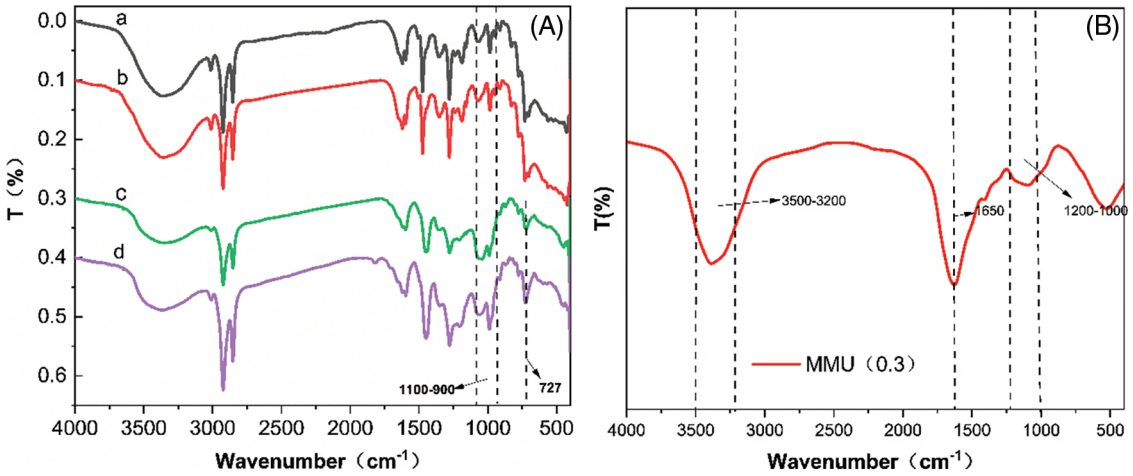

Figure 4: FT-IR spectra curves of RL, LMU1-3 wt% and MMU. (a) RL sap, (b) LMU1-3% sap, (c) RL film, (d) LMU1-3% film, (B) MMU

By observing the curves of Fig. 4A, the absorption peak of films at 2800–2975 cm^{-1} was obviously stronger than that of sap, and the peak of 988 cm^{-1} disappeared. It illustrated that the curing of the RL was mainly due to the urushiol free radical attacking the double bond to form polymer. It can be seen from Figs. 4c and 4d, a new peak at 900–1100 cm^{-1} was assigned to C-C vibration, and the peak intensity of LMU1-3% is greater than that of RL. This can be explained that urushiol can react with N-H in MMU to form C-N. Another new peak at 727 cm^{-1} was seen in Fig. 4d, which was due to the formation of a benzene ring linger between MMU and urushiol, as shown in Scheme 1 [32].

3.5 NMR Analysis

The ^{13}C NMR of RL, LMU1-3% were presented in Fig. 5. In the spectrum of the RL, the signal 110–140 ppm was corresponding to the aromatic carbon on the benzene ring [33–35]. The signal of 130–135 ppm was assigned to the olefins in the side chain. It can be seen from the figure that there were mainly three olefins, all of which were conjugated alkatriene, which was consistent with the results of FT-IR analysis. Consult the literature to know that the basic structure of urushiol was shown in Scheme 2. In Fig. 5, the spectra of the RL shifted to the low field, and the abundance of the peaks was also reduced. The small amount peaks at 71–73 ppm were assigned to the dendritic methylol groups in methylolurea [36]. In Fig. 5, the chemical peak at 77 ppm was shifted to the high filed and the abundance of the peak increased. This peak was originally assigned to the chemical shift of $CDCl_3$, while this location related to the methylene methyl ethers in MMU, which indicated that the main methylol groups in MMU were successfully transformed into methylene methyl ethers by the self-condensation or the co-polycondensation reaction with the increase of the temperature, as shown in Tables 5 and 6. Therefore, the chemical shift of methylene methyl ethers and $CDCl_3$ overlapped leading to the increase of this peak [37]. In the LMU1-3% curve, the abundance of the peak at 110–140 ppm was significantly less than that of RL, indicating that the olefins on the urushiol side chain in LMU1-3% were reduced, while the abundance of the peak at 10–40 ppm was significantly increased. This phenomenon can be speculated that the olefin on the urushiol side chain was reduced to form a C-C bond. The chemical shift of the ether bond did not appear in the curve, indicating that the ether bond was not generated, and FT-IR analysis speculated that the C-N bond could not be detected in NMR analysis. From Fig. 5, it can be seen that the peaks at 18–35 ppm and 125–150 ppm of LMU1-3% are obviously shifted to the high field, which is due to the presence of 6 π electrons on the benzene ring, forming an external the magnetic field, where the C atoms attached to the benzene ring are out of alignment with the external magnetic field, has a shielding effect, resulting in high field displacements.

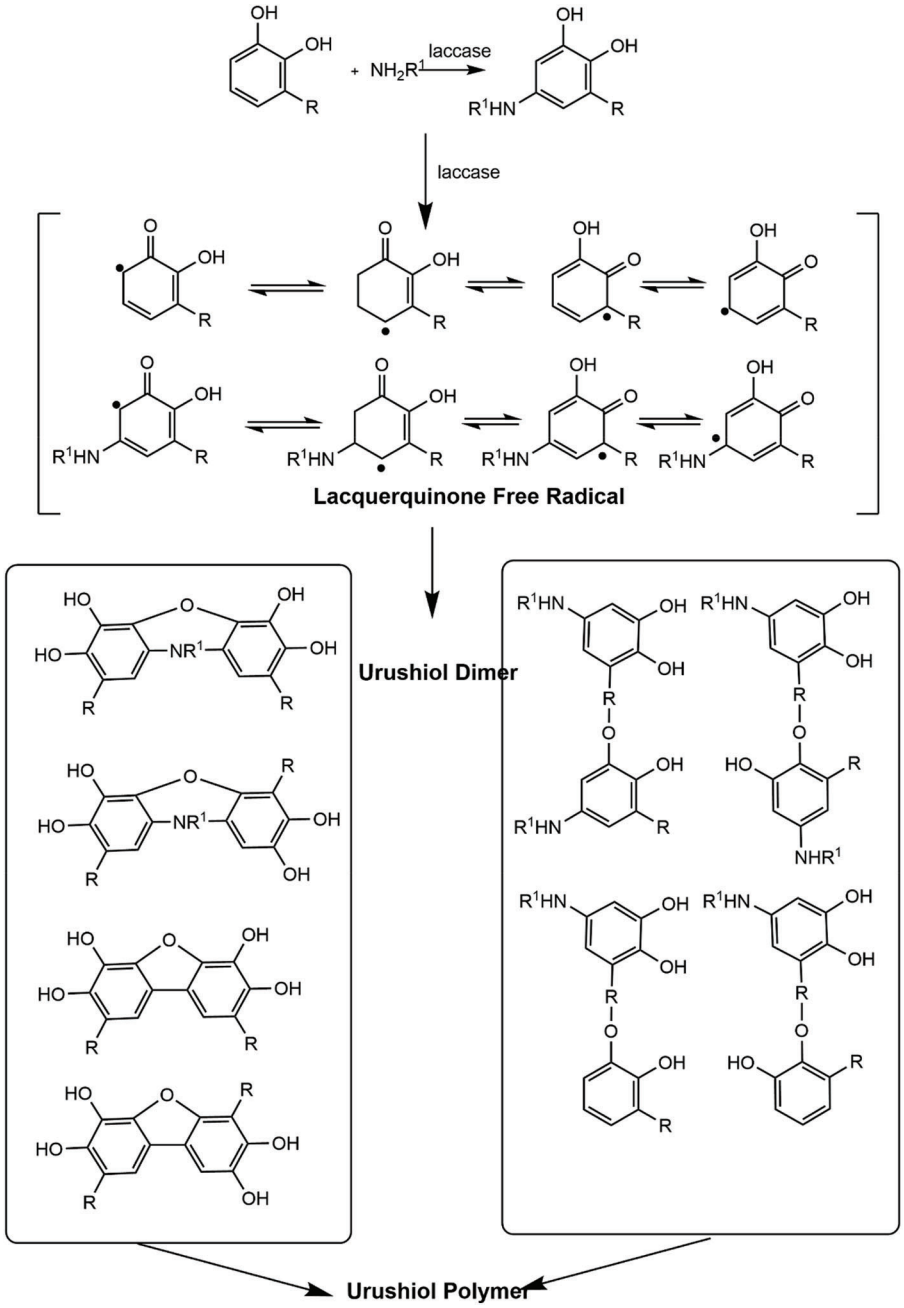

Scheme 1: The reaction of urushiol with MMU

3.6 SEM Analysis

The SEM images of RL and LMU films with different loading level were shown in Fig. 6. It was noticed that there were some "caves" on all films, mainly due to the evaporation of waterdrops during the drying process. The diameter of the pores on the RL film is 2–4 um [2,3,10]. When the amount of MMU is less than 3%, the number of caves on the modified film is less and the diameter is smaller, and the surface is smoother. When the addition amount of MMU is 3%, the surface shape of the film is the best. However, when addition amount of MMU are 5 wt% and 7 wt%, the diameter of "caves" on the LMU were bigger than that of the RL. This result was basically consistent with the performance of the basic performance.

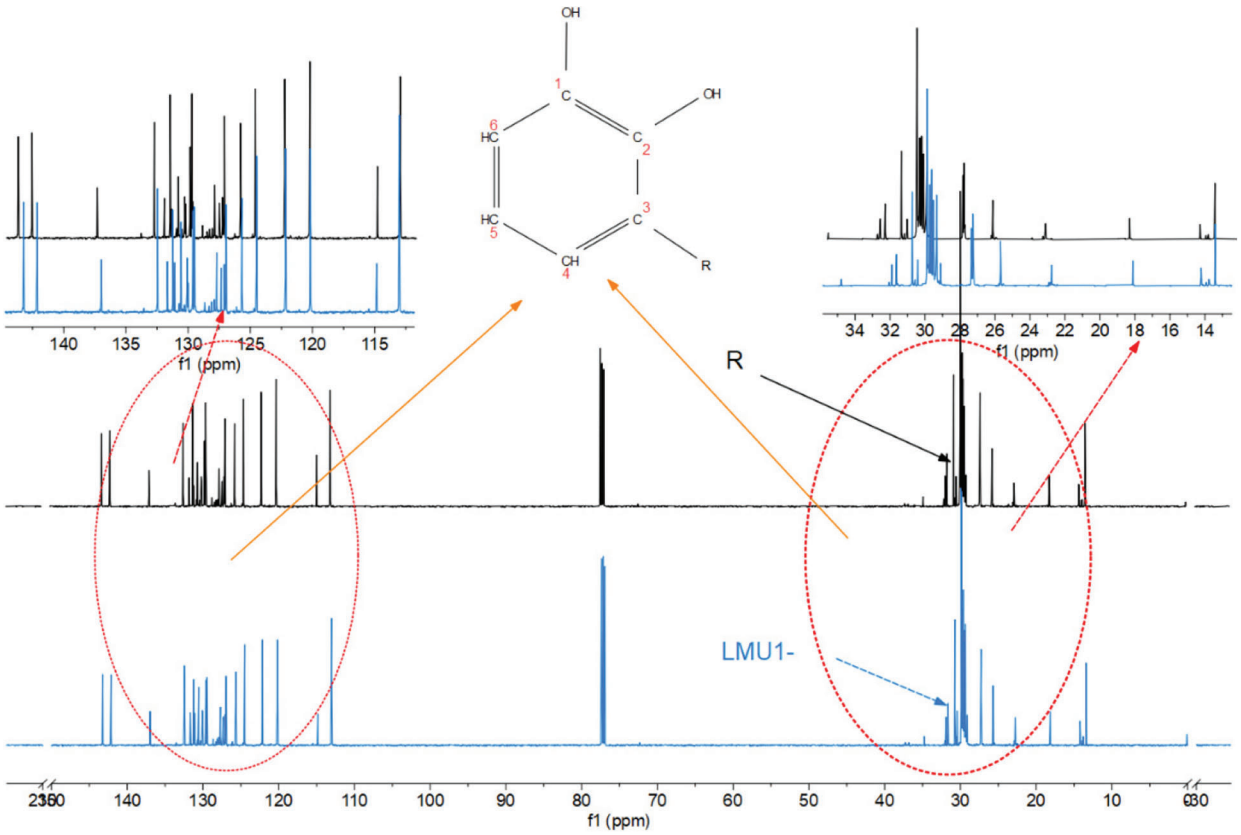

Figure 5: ^{13}C NMR spectra of original and modified lacquer

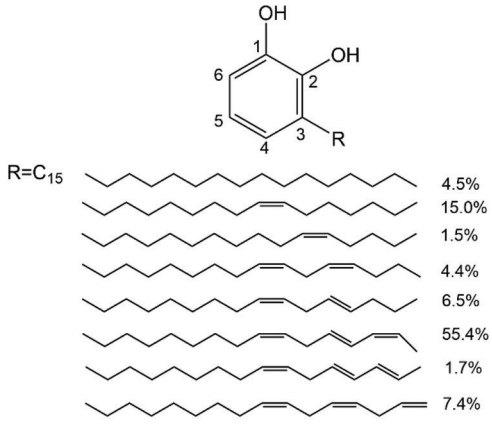

Scheme 2: The structure of urushiol

Table 5: The chemical shifts of main urushiol of lacquer

The chemical structure of lacquer		Chemical shifts (ppm)
1		144.5
2		143.04
3		129.61
4		121.43
5		120.25
6		113.34
R	-CH_2-	29–32
	-C=C-	127–137

Table 6: The chemical shifts of urea formaldehyde resin [38,39]

The chemical structure of resin		Chemical shifts
Methylene linkages	$HNCH_2NH$	44~47
	$HNCH_2N(CH_2)$	51~55
	$N(CH_2)CH_2N(CH_2)$	60~62
Methylol groups	$HNCH_2OH$	63.5~65
	$N(CH_2)CH_2OH$	71~73
	$N(CH_2OH)_2$	
Methylene methyl ethers	$HNCH_2OCH_3$	73~75.2
	$N(CH_2)CH_2OCH_3$	77.7~78.2
	Uron-CH_2OCH_3	77.2~77.5
Dimethylene ether linkages	$HNCH_2OCH_2NH$	69~70.2
	$HNCH_2OCH_2N(CH_2)$	
Hemiformal of methylol groups	$NHCH_2OCH_2OH$	66~69
	$NHCH_2OCH_2OH$	86~87
	$N(CH_2)CH_2OCH_2OH$	
Free formaldehyede		82

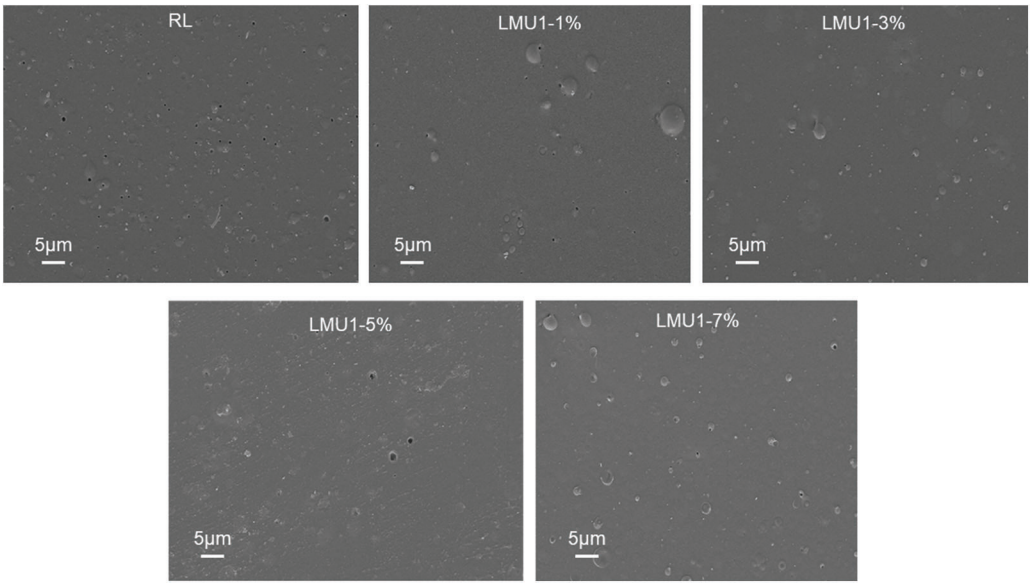

Figure 6: The SEM images of RL and LMU films with different loading level

4 Conclusion

In this study, MMU was synthesized with different molar ratio of formaldehyde and urea (F/U), the molar ratio and addition amount of MMU were optimized by the comprehensive properties of the modified RL. And the chemical structure of the RL before and after modification was analyzed by FT-IR and NMR. The results indicated the comprehensive performance of LMU increase with the decrease of molar ratio of MMU. The optimal addition amount of LMU1 is 3.0%, the hardened dry time, gloss, pencil hardness and impact resistance of which were significantly better than those of RL. The TG, FT-IR and ^{13}C NMR analysis revealed that the improvement of comprehensive properties of RL film was mainly due to the structures of the RL were significantly improved by cross-linking with the hydroxymethyl groups and methylene methyl ethers of MMU and the surface smoothness of the lacquer film had also been improved. This modified lacquer facilitates the use on ceramics, artwork and exterior architecture.

Acknowledgement: The authors also thank Shiyanjia Lab (www.shiyanjia.com) for the SEM, TG, FT-IR and NMR analysis.

Author Contributions: Conceptualization, Y. C.; Methodology, Q. X, Y. T., and H. T.; Validation, Q. X., Y. T., and H. T.; Data Curation, Q. X. and Y. T.; Writing-Original Draft, Q. X.; Investigation, Q. X., J. L., M. C., and H. X.; Resources, Q. X., H. T., Q. F., X. G., J. L., H. X., and M. C.; Software, Q. X., Y. T., H. T., J. L., H. X., and M. C.; Writing-Review & Editing, Y. T. and Y. C.; Supervision, Y. T.; Project Administration, Y. T.; Formal Analysis, Y. C.; Funding Acquisition, Y. C. and M. C. All authors have read and agreed to the final version of the manuscript submitted for publication.

Funding Statement: This work would like to thank the M. C. support by Key Research and Development Project of Sichuan Science and Technology Plan Projects (Grant No. 2020YFS0357), Ministry of Education Humanities and Social Sciences Research Project of China (Grant No. 19YJC760009), Research Program of Science and Technology Agency of Sichuan of China (Project No. 2012129068) and Research Interest in Training Program of Sichuan Agricultural University (Project No. 2021182).

Conflicts of Interest: The authors declare that they have no conflicts of interest to report regarding the present study.

References

1. Lu, R., Yoshida, T., Miyakoshi, T. (2013). Oriental lacquer: A natural polymer. *Polymer Reviews, 53(2),* 153–191. DOI 10.1080/15583724.2013.776585.
2. Yang, J., Deng, J., Zhang, Q., Shen, Q., Li, D. et al. (2015). Effects of polysaccharides on the properties of Chinese lacquer sap. *Progress in Organic Coatings, 78(3),* 176–182. DOI 10.1016/j.porgcoat.2014.09.007.
3. Zhang, D., Xia, J., Xue, H., Zhang, Y., Lin, Q. (2020). Improvement on properties of Chinese lacquer by polyamidoamine. *Polymer Engineering & Science, 60(6),* 1177–1185. DOI 10.1002/pen.25371.
4. Xia, J., Lin, J., Xu, Y., Chen, Q. (2011). On the UV-induced polymeric behavior of Chinese lacquer. *ACS Applied Materials & Interfaces, 3(2),* 482–489. DOI 10.1021/am1010578.
5. Chang, C., Lee, H., Lu, K. (2018). Manufacture and characteristics of oil-modified refined lacquer for wood coatings. *Coatings, 9(1),* 11. DOI 10.3390/coatings9010011.
6. Wan, Y., Lu, R., Akiyama, K., Okamoto, K., Honda, T. et al. (2010). Effects of lacquer polysaccharides, glycoproteins and isoenzymes on the activity of free and immobilised laccase from *Rhus vernicifera*. *International Journal of Biological Macromolecules, 47(1),* 76–81. DOI 10.1016/j.ijbiomac.2010.03.016.
7. Lu, R., Honda, T., Ishimura, T., Miyakoshi, T. (2005). Study of a naturally drying lacquer hybridized with organic silane. *Polymer Journal, 37(4),* 309–315. DOI 10.1295/polymj.37.309.
8. Tamburini, D., Bonaduce, I., Colombini, M. P. (2015). Characterization and identification of urushi using in situ pyrolysis/silylation-gas chromatography-mass spectrometry. *Journal of Analytical and Applied Pyrolysis, 111,* 33–40. DOI 10.1016/j.jaap.2014.12.018.
9. Yang, J., Deng, J., Zhu, J., Liu, W., Zhou, M. et al. (2016). Thermal polymerization of lacquer sap and its effects on the properties of lacquer film. *Progress in Organic Coatings, 94(1),* 41–48. DOI 10.1016/j.porgcoat.2016.01.021.
10. Yang, J., Deng, J., Zhu, J., Shen, Q., Li, D. (2015). Lacquer sap with reactive maleic hemiester surfactant-modified phase interface and its properties. *Progress in Organic Coatings, 87(12),* 138–145. DOI 10.1016/j.porgcoat.2015.05.027.
11. Xia, J., Xu, Y., Lin, J. (2010). UV-induced polymerization of urushiol. II: Effects of hydrogenation degree of urushiol on surface morphology. *Progress in Organic Coatings, 67(3),* 365–369. DOI 10.1016/j.porgcoat.2009.12.004.
12. Xia, Z., Miyakoshi, T., Yoshida, T. (2004). Lipoxygenase-catalyzed polymerization of phenolic lipids suggests a new mechanism for allergic contact dermatitis induced by urushiol and its analogs. *Biochemical and Biophysical Research Communications, 315(3),* 704–709. DOI 10.1016/j.bbrc.2004.01.112.
13. Zhang, L., Wu, H., Zheng, Z., He, H., Wei, M. et al. (2019). Fabrication of graphene oxide/multi-walled carbon nanotube/urushiol formaldehyde polymer composite coatings and evaluation of their physico-mechanical properties and corrosion resistance. *Progress in Organic Coatings, 127,* 131–139. DOI 10.1016/j.porgcoat.2018.10.026.
14. Xu, Y., Tong, Z., Xia, J., Hu, B., Lin, J. (2011). Urushiol-formaldehyde polymer microporous films with acid-alkali resistance property: Effects of formation conditions on surface morphologies. *Progress in Organic Coatings, 72(3),* 586–591. DOI 10.1016/j.porgcoat.2011.06.018.
15. Zhang, L., Wang, W., Wu, H., Zheng, Z., Wei, M. et al. (2021). Corrosion-resistant composite coatings based on a graphene oxide-metal oxide/urushiol formaldehyde polymer system. *Journal of Coatings Technology and Research, 18(5),* 1209–1225. DOI 10.1007/s11998-021-00480-2.
16. Lu, R., Wan, Y., Honda, T., Ishimura, T., Kamiya, Y. et al. (2006). Design and characterization of modified urethane lacquer coating. *Progress in Organic Coatings, 57(3),* 215–222. DOI 10.1016/j.porgcoat.2006.08.014.
17. Yang, J., Zhu, J., Liu, W., Deng, J., Ding, Y. (2015). Prepolymerization of lacquer sap under pure oxygen atmosphere and its effects on the properties of lacquer film. *International Journal of Polymer Science, 2015,* 517202. DOI 10.1155/2015/517202.

18. Yang, J., Zhu, J., Shen, F., Cai, J., Zhou, M. (2018). Promotion by copper (II)-modified montmorillonite of the drying property of oriental lacquer sap. *Progress in Organic Coatings, 118(1),* 72–81. DOI 10.1016/j.porgcoat.2018.01.023.
19. Lu, R., Harigaya, S., Ishimura, T., Nagase, K., Miyakoshi, T. (2004). Development of a fast drying lacquer based on raw lacquer sap. *Progress in Organic Coatings, 51(3),* 238–243. DOI 10.1016/j.porgcoat.2004.08.006.
20. Lu, R., Ebata, N., Zhang, F., Miyakoshi, T. (2014). Development of a new type lacquer based on *Rhus vernicifera* sap with chitosan. *Progress in Organic Coatings, 77(2),* 439–443. DOI 10.1016/j.porgcoat.2013.11.006.
21. Lu, R., Ishimura, T., Tsutida, K., Honda, T., Miyakoshi, T. (2005). Development of a fast drying hybrid lacquer in a low-relative-humidity environment based onkurome lacquer sap. *Journal of Applied Polymer Science, 98(3),* 1055–1061. DOI 10.1002/(ISSN)1097-4628.
22. Chen, Y., Fan, D., Qin, T., Chu, F. (2014). Thermal degradation and stability of accelerated-curing phenol-formaldehyde resin. *BioResources, 9(3),* 4063–4075. DOI 10.15376/biores.9.3.4063-4075.
23. Ikizer, B., Lawton, C. W., Orbey, N. (2021). Poly(para-phenylene) fibers–Characterization and preliminary data for conversion to carbon fiber. *Polymer, 228,* 123945. DOI 10.1016/j.polymer.2021.123945.
24. Zhang, Z., Liu, Y., Shui, X., Yu, Y., Zheng, C. et al. (2021). Free radical polymerization of acrylates bearing acetylene for preparation of clickable polymers. *Polymer, 228(8),* 123906. DOI 10.1016/j.polymer.2021.123906.
25. Ikenaga, M., Tachibana, Y., Kitajima, S. (2020). Curing of Urushi under basic pH conditions by a dual enzyme system. *Progress in Organic Coatings, 138,* 105429. DOI 10.1016/j.porgcoat.2019.105429.
26. He, J., Chen, Q., Huang, H., Zheng, L., Chen, B. et al. (2015). Development of novel anisotropic Janus composite particles based on Urushiol-iron/polystyrene polymer. *Progress in Organic Coatings, 85,* 15–21. DOI 10.1016/j.porgcoat.2014.09.023.
27. Lee, B., Kim, H. (2004). Curing behaviors of Korean Dendropanax lacquer determined by chemical and physical measures. *Journal of Applied Polymer Science, 92(1),* 625–630. DOI 10.1002/(ISSN)1097-4628.
28. Jdidi, H., Fourati, N., Zerrouki, C., Ibos, L., Fois, M. et al. (2021). Exploring the optical and dielectric properties of bifunctional and trifunctional epoxy polymers. *Polymer, 228(9),* 123882. DOI 10.1016/j.polymer.2021.123882.
29. Hassan, N., Singh, M., Sulaiman, S., Jain, P., Sharma, K. et al. (2019). Molecular docking-guided ungual drug-delivery design for amelioration of onychomycosis. *ACS Omega, 4(5),* 9583–9592. DOI 10.1021/acsomega.9b00436.
30. Niimura, N., Miyakoshi, T. (2006). Structural study of oriental lacquer films during the hardening process. *Talanta, 70(1),* 146–152. DOI 10.1016/j.talanta.2005.12.039.
31. Ishimura, T., Lu, R., Yamasaki, K., Miyakoshi, T. (2010). Development of an eco-friendly hybrid lacquer based on kurome lacquer sap. *Progress in Organic Coatings, 69(1),* 12–15. DOI 10.1016/j.porgcoat.2010.04.019.
32. Rong, L., Miyakoshi, T. (2015). Modification of lacquer. *Lacquer Chemistry and Applications, 3(318–322),* 171–214. DOI 10.1016/B978-0-12-803589-4.00010-9.
33. Xia, J., Xu, Y., Hu, B., Lin, J. (2009). A rapid approach to urushiol-copper(I) coordination polymer under UV irradiation. *Progress in Organic Coatings, 65(4),* 510–513. DOI 10.1016/j.porgcoat.2009.04.006.
34. Lu, R., Kamiya, Y., Kumamoto, T., Honda, T., Miyakoshi, T. (2006). Deterioration of surface structure of lacquer films due to ultraviolet irradiation. *Surface and Interface Analysis, 38(9),* 1311–1315. DOI 10.1002/sia.2451.
35. Kanehashi, S., Oyagi, H., Lu, R., Miyakoshi, T. (2014). Development of bio-based hybrid resin, from natural lacquer. *Progress in Organic Coatings, 77(1),* 24–29. DOI 10.1016/j.porgcoat.2013.07.013.
36. Behera, S., Patra, B. N. (2021). One-pot synthesis of β-amino carbonyl compounds under solvent free condition by using alum doped nanopolyaniline catalyst. *Polymer, 228(5),* 123851. DOI 10.1016/j.polymer.2021.123851.
37. Wang, N., Liu, J., He, L., Zhou, T., Rong, B. et al. (2014). Characterization of Chinese lacquer in historical artwork by on-line methylation pyrolysis-gas chromatography/mass spectrometry. *Analytical Letters, 47(15),* 2488–2507. DOI 10.1080/00032719.2014.913172.
38. Siimer, K., Kaljuvee, T., Christjanson, P., Pehk, T. (2005). Changes in curing behaviour of aminoresins during storage. *Journal of Thermal Analysis and Calorimetry, 80(1),* 123–130. DOI 10.1007/s10973-005-0623-8.
39. Liu, Y. (2006). The curing agent systems and curing characteristics for urea-formaldehyde resin with low formaldehyde emission. *China Adhesives, 15(10),* 42. DOI 10.13416/j.ca.2006.10.01.